Schottky barrier lowering in n-AlGaAs/GaAs/AlGaAs double-heterojunction by local light illumination

Takuya Kawazu
National Institute for Materials Science, Tsukuba, Ibaraki 305-0047, Japan
*E-mail: KAWAZU.Takuya@nims.go.jp

Abstract: We investigated the wavelength dependence of the Schottky photocurrent (I_{SG}) in an n-AlGaAs/GaAs/AlGaAs double-heterojunction under local light illumination. I_{SG} was measured with the illumination from two light sources (Light A and B). Light A illuminated the entire Schottky gate region at 60 μW/mm² with varying the wavelength (940, 975, and 1064 nm), while Light B (670 nm laser) locally illuminated the ungated region at power levels (P_B) ranging from 0 to 2.9 μW. At low P_B (≤ 86 nA) and high P_B (≥ 0.14 μW), I_{SG} increases and decreases respectively with the increasing photon energy of Light A. By analyzing the experimental data using a hot carrier model, this behavior is attributed to the Schottky barrier lowering induced by Light B. The reduction in the effective Schottky barrier height increases with increasing P_B, reaching about 0.5 – 0.6 eV.

1. Introduction

Owing to the importance in photodetector applications, the infrared (IR) photoresponses of Schottky barrier diodes have attracted strong interest for a few decades.[1-23] A Schottky potential barrier develops in the interface region of a metal film on a semiconductor.[24] When incident photons are absorbed through free-carrier transitions in the metal film,[25] photo-carriers are generated and transfer to the semiconductor, resulting in the generation of a photocurrent. The detectable photon energy is determined by the Schottky barrier height, not by the semiconductor bandgap, in which the IR photo-sensing is potentially possible in the energy rage of 0.2 – 0.6 eV by choosing an appropriate combination of a metal and a semiconductor.[5,6,9,25] Various efforts have been made to improve the photoresponses of Schottky-barrier diodes, such as back illuminations,[6,9,10] very thin metal gates,[5),6),9] two Schottky-barriers,[17] gate edge illuminations,[19,21] surface plasmon,[14)-16] and optical cavities.[6,11,12]

In our previous studies,[22,23] we investigated the Schottky photocurrent in n-AlGaAs/GaAs and n-AlGaAs/GaAs/AlGaAs heterojunctions with metal gates. We observed that the photocurrent induced by illuminating the Schottky gate region is significantly enhanced when the ungated region is also illuminated. This enhancement is attributed to holes excited by the illumination of the ungated region, which diffuse in the GaAs buffer layer and subsequently reach the Schottky gate region. Although the model proposing that holes contribute to the enhancement of the Schottky photocurrent has successfully explained the experimental results, the precise mechanism through which these holes influence the photocurrent remains unclear.

In this work, we investigate the Schottky photocurrent I_{SG} in an n-AlGaAs/GaAs/AlGaAs double-heterojunction under two light sources (Light A and B in Fig. 1). Light A was used to illuminate the entire Schottky gate region with varying its wavelength, while Light B was employed to selectively illuminate the ungated region with modulating the power levels P_B. By analyzing I_{SG} using a hot carrier model, we show that the illumination of the Light B has an effect equivalent to reducing the effective Schottky-barrier height. As P_B increases, the reduction $\delta\Phi$ in the effective Schottky barrier height increases, with $\delta\Phi$ reaching approximately 0.5 – 0.6 eV.

2. Experimental methods

By using molecular beam epitaxy, we prepared the heterojunction sample on a semi-insulating GaAs(100) substrate. We grew a 500-nm-thick GaAs buffer layer, a superlattice layer (25 periods of 10 nm $Al_{0.27}Ga_{0.73}As$/2 nm GaAs), a 15-nm-thick GaAs quantum well (QW) channel, a 10-nm-thick nondoped AlGaAs spacer, an 80-nm-thick Si-doped AlGaAs layer, and a 10-nm-thick GaAs capping layer. Throughout the growth, the substrate temperature was set at 580 °C. Schematic drawings of the sample cross-section view and the band diagram are illustrated in Figs. 2 and 3.

The heterojunction sample was processed into a Hall bar device with a Schottky gate. The Hall bar structure (represented by the dot-patterned region in Fig. 4) was defined using photolithography, followed by wet etching. To form the Schottky metal gate, aluminum was deposited via vacuum evaporation to a thickness of approximately 100 nm (gray region in Fig. 4). The Schottky gate region of the heterojunction, indicated by the broken-line boundary, has a width (W) of 50 μm and a length (L) of 550 μm. The ohmic contacts between the electrode pads and the QW channel (hatched circles in Fig. 4) were made by alloying InSn at 400 °C for 2 minutes in an argon atmosphere. The sample was bonded using silver paste in a ceramic package with a gold-plated surface.

Photocurrent measurements were performed at room temperature using the experimental setup with the schematic of device connections depicted in Figs. 1 and 4. The Schottky photocurrent (I_{SG} in Figs. 1 and 4) from the source contact (S) to the Schottky metal gate (G) was monitored using a source measure unit (Keithley 2635), capable of measuring DC currents in the range of 0.1 fA to 1.53 A.

For the illuminate of the Schottky gate region, we used 940-, 975-, and 1064-nm laser beams (Light A), and the entire heterojunction structure was irradiated by one of them with an excited power density of about 60 μW/mm^2. Since the photon energy of Light A is below the bandgap energy of GaAs and AlGaAs, interband absorption does not occur, resulting in GaAs and AlGaAs crystals being nearly transparent to the incident light. Consequently, Light A has minimal influence in the ungated region, even though it illuminates the entire structure. Light A reaches the Schottky metal-semiconductor interface either through transmission via the gate metal or by reflection at the back surface, subsequently exciting electrons (Fig. 2). The excited electrons then transfer to the QW, inducing the Schottky photocurrent I_{SG}.

For the illumination of the ungated region, we used a 670-nm-laser beam (Light B). Light B was focused by a microscope objective lens, allowing the observation of the sample surface and precise monitoring of the irradiation position. The laser spot, with a diameter of approximately 50 μm, was positioned at the location indicated by 'L' in Fig. 4, about 1.4 mm from the Schottky gate region. The photon energy of Light B, approximately 1.85 eV, exceeds the bandgap energies of the n-$Al_{0.27}Ga_{0.73}As$ layer (~1.78 eV), the GaAs buffer layer, and the superlattice layer, resulting in absorption processes within these layers. However, the absorption in the superlattice layer is expected to be the most significant process for enhancing the Schottky photocurrent.[23] When Light B is absorbed by the superlattice layer, it generates electrons and holes (Fig. 3). The electrons migrate towards the QW and are rapidly and uniformly redistributed within the QW due to the high conductivity of the two-dimensional electron gas (2DEG) channel. In contrast, the generated holes move toward the GaAs buffer layer and accumulate there. The accumulated holes diffuse laterally and then reach the Schottky gate region. The positive charge of the holes induces electric fields, thereby enhancing the Schottky photocurrent I_{SG} under the illumination of Light A.

3. Results and Discussion

3.1 Experimental results

Initially, the Schottky photocurrent I_{SG} from the source contact (S) to the metal gate (G) was measured under the conditions where the wavelength λ_A of Light A was 940 nm, and the power P_B of Light B was 0.57 μW. Figure 5 shows I_{SG} for the on/off action of Light A and B. 'A', 'B', and 'A+B' in the horizontal axis of Fig. 5 indicate the illuminations of Light A, Light B, and both, respectively. 'off' represents that all the lights are off. When Light A irradiates the sample ('A' in Fig. 5), the Schottky photocurrent flows from S to G, where I_{SG} is positive. Upon irradiation with Light A, photoelectrons are excited at the Schottky metal-semiconductor interface and subsequently transfer to the QW channel (Fig. 2), resulting in the generation of the photocurrent from S to G. For the illumination of Light B only ('B' in Fig. 5), the Schottky photocurrent is not generated (I_{SG} ~ 0). Light B excites electrons and holes (Fig. 3), but the electron-hole excitation itself does not induce the Schottky photocurrent. When both Light A and B simultaneously illuminate the heterojunction ('A+B' in Fig. 5), I_{SG} increases by a factor of 4 compared to Light A only. Note that the IR photoresponse in the Schottky gate region is effectively enhanced by the illumination of Light B, where the illumination position is far away (~ 1.4 mm) from the gate region. Due to the separation of holes from the electrons that recombine with them by a thick superlattice, the photo-generated and subsequently accumulated holes diffuse laterally in the GaAs buffer layer over a significant distance, allowing them to reach the Schottky gate region (Fig. 3). I_{SG} under Light A illumination is enhanced by the electric fields induced by the positive hole charge in the Schottky gate region.

A similar measurement was conducted with Laser B positioned at the GaAs substrate location marked as L' in Fig. 4. As indicated by the dotted line in Fig. 5, no increase in the photocurrent for Light A was observed when exposed to Light B. This observation confirms that the photocurrent increase is not due to substrate illumination or stray light, but requires electron-hole excitation of the heterojunction by Light B.

Figure 6 shows the Schottky photocurrent I_{SG} from S to G when the wavelength of Light A is 940, 975, and 1064 nm. Here, the power P_B of Light B is 20 nW. I_{SG} are approximately 1.6, 3.1, and 3.6 nA for Light A illumination of 1064-, 975-, and 940-nm wavelengths, respectively ('A' in Fig. 6). When both Light A and B simultaneously illuminate the heterojunction ('A+B' in Fig. 6), I_{SG} increase and are about 4.7, 5.8, and 6.2 nA for the 1064-, 975-, and 940-nm laser illuminations.

Figure 7 shows the Schottky photocurrent I_{SG} when the power P_B of Light B is about 0.86 μW. The other experimental conditions are the same as those in Fig. 6. When Light A and B simultaneously illuminate the heterojunction ('A+B' in Fig. 7), I_{SG} are about 19.2, 16.4, and 14.5 nA for the 1064-, 975-, and 940-nm laser illuminations. The values of I_{SG} are significantly higher than when P_B = 20 nW ('A+B' in Fig. 6), which is due to the excitation of a larger number of holes. Note that I_{SG} increases with increasing λ_A at P_B = 0.86 μW, while I_{SG} shows a downward trend with increasing λ_A at P_B = 20 nW.

Next, we examined the Schottky photocurrent I_{SG} by altering the wavelength λ_A of Light A and the power P_B of light B, with both Light A and B concurrently illuminating the heterojunction. Figure 8 shows I_{SG} as a function of the photon energy ($h\nu_A = hc/\lambda_A$, where h represents Planck's constant and c denotes the speed of light) of Light A. Here, the experimental conditions are identical to those previously described, with the exception of P_B. Note that as $h\nu_A$ increases, I_{SG} increases and decreases at $P_B \leq 86$ nA and ≥ 0.14 μW. When

λ_A is 1064 nm (~ 1.17 eV), 975 nm (~ 1.27 eV), and 940 nm (~ 1.32 eV), I_{SG} increase about 14.3, 6.5, and 5.1 times respectively with the increase in P_B from 0 (red open circles) to 2.9 μW(gray inverted triangles); the smaller the photon energy of Light A is, the stronger the enhancement effect of Light B becomes.

3.2 Schottky barrier lowering

According to a hot carrier model,[17] the Schottky photocurrents I_{SG} is given by

$$I_{SG} = \frac{eAP_A}{2h\nu_A}\left(1 - \sqrt{\frac{\Phi}{h\nu_A}}\right)^2 \qquad (1)$$

where e is the elementary charge, A is the optical absorptance, Φ is the effective Schottky barrier height, and P_A is the incident optical power. In our case, P_A corresponds to the power of Light A and is about 60 μW/mm^2×LW. The solid lines in Fig. 8 represent I_{SG} derived from Eq. (1), using Φ as a fitting parameter to match the experimental data corresponding to each power level P_B of Light B. The value of AP_A is set to 7×10^{-8} W (A ~ 0.042) and is determined such that Φ (≡ Φ_0) is 0.6 eV in the absence of Light B irradiation. The effective Schottky barrier height Φ_0 (= 0.6 eV) under dark conditions is an estimate derived from the J_{SG}-V_G characteristics observed when a bias voltage V_G is applied to the Schottky gate. The optical absorptance A of 0.042 indicates that only 4.2% of the incident light contributes to photocarrier generation. The low efficiency is primarily attributed to the high reflectivity of the Schottky metal gate, where the 100-nm-thick aluminum layer is expected to reflect over 90% of the incident light. Improving efficiency can be achieved by reducing the thickness of the metal gate and/or selecting an alternative gate material.

As shown by the solid lines in Fig. 8, the dependence of the measured Schottky photocurrent I_{SG} on the photon energy $h\nu_A$ is well described by Eq. (1), with Φ being adjusted for each power level P_B of Light B. Notably, the transition of I_{SG} from an increasing to a decreasing trend as a function of $h\nu_A$ can be attributed to variations in Φ. For a fixed excitation power P_A of the Light A, the number of incident photons decreases inversely with increasing $h\nu_A$, as described by the term $AP_A/h\nu_A$ in Eq. (1). Conversely, the fraction of photo-excited electrons that surmount the Schottky barrier increases with increasing $h\nu_A$, where the fraction is given by the term $\left(1 - \sqrt{\Phi/h\nu_A}\right)^2/2$ in Eq. (1). The overall trend whether increasing or decreasing of I_{SG} as a function of $h\nu_A$ is determined by the interplay of these two factors. Differentiating Eq. (1) with respect to $h\nu_A$ reveals that I_{SG} increases with $h\nu_A$ for $h\nu_A < 4\Phi$, whereas it exhibits a decreasing trend for $h\nu_A > 4\Phi$.

Although the hot electron model (Eq. (1)) qualitatively aligns with the experimental data presented in Fig. 8, its quantitative accuracy remains unsatisfactory. Specifically, the measured Schottky photocurrent I_{SG} increases with increasing the photon energy $h\nu_A$ under illumination with Light B at P_B = 86 and 57 nW (black and pink open triangles in Fig. 8). In contrast, the hot electron model predicts an inverse trend (black and pink solid lines in Fig. 8). This discrepancy primarily arises from an error in estimating the effective Schottky barrier height Φ_0 (= 0.6 eV) under dark conditions, which will be discussed in the following section. Furthermore, the deviation between the model predictions and experimental results can be attributed to factors such as measurement uncertainties (estimated error in I_{SG} of approximately 5 – 6%) and simplifications inherent in the hot electron model, as well as the omission of electron photo-excitation in the QW[23] and the wavelength dependence of the optical absorptance A. The solid circles in Fig. 9 represent the effective Schottky barrier height Φ, determined via the fitting procedure described above, plotted as a function of the excitation power P_B of Light B. As P_B increases from 0 to 2.9 μW, Φ decreases from approximately 0.6 to 0.03 eV. It should be noted that the reliability of these values requires careful consideration, as the obtained value of Φ is highly sensitive to the estimation error of Φ_0 under dark conditions. A discussion of this issue will be provided in the following section. To mitigate this uncertainty, we conduct our analysis using the effective Schottky barrier reduction $\delta\Phi \equiv \Phi_0 - \Phi$, which is less influenced by the magnitude of Φ_0 (see the following section). The solid circles in Fig. 10 represent the effective Schottky barrier reduction $\delta\Phi$ as a function of the excitation power P_B of Light B. As P_B increases, $\delta\Phi$ increases, and the maximum reduction in the effective Schottky barrier height is about 0.5 – 0.6 eV. In a Schottky barrier diode, the barrier energy is governed by the work function of the gate metal, the electron affinity of the semiconductor, and the surface states at the metal-semiconductor interface. For many III-V compounds, the Schottky barrier energy is predominantly determined by the surface states. The intrinsic energy Φ_{int} of such a Schottky barrier is reduced by the image charge of the electrons emitted in an electric field. The lowering $\Delta\Phi_0$ in Schottky barrier energy is proportional to the square root of the electric field E_0 present at the semiconductor side of the Schottky metal-semiconductor interface, as expressed by

$$\Delta\Phi_0 = \sqrt{\frac{eE_0}{4\pi\varepsilon_S}}, \quad (2)$$

where ε_s is the permittivity of the semiconductor. For a Schottky diode with a barrier height of 0.6 eV, $\Delta\Phi_0$ is estimated to be about 0.057 eV. Note that Φ_0 defined above corresponds to Φ_{int}-$\Delta\Phi_0$. When the heterojunction is irradiated with Light B, photo-excited holes move toward the substrate and diffuse to the Schottky gate region (Figs. 1 and 3), and their positive charge induces an electric field E_{ind} in addition to E_0 in Eq. (2). Such an electric field causes an additional lowering $\delta\Phi$ of the Schottky barrier energy. E_{ind} is anticipated to be proportional to the hole density, which is expected to be proportional to the excitation power P_B of Light B, resulting in

$$\frac{eE_{ind}}{4\pi\varepsilon_S} = \alpha P_B, \quad (3)$$

where α is a constant with a dimension of J·s. From Eqs. (2) and (3), we obtain

$$\Delta\Phi_0 + \delta\Phi = \sqrt{\frac{e(E_0+E_{ind})}{4\pi\varepsilon_S}} = \sqrt{\Delta\Phi_0^2 + \alpha P_B}. \quad (4)$$

The solid line in Fig. 10 represents Eq. 4 with $\Delta\Phi_0$ set to 0.057 eV and α as the fitting parameter. At low power P_B (<~ 0.06 μW) of Light B, Eq. 4 agrees with the experimental data for $\alpha = 5.9\times10^{-13}$ eV·s, indicating the validity of our explanation. In contrast, at high P_B (>~ 0.1 μW), the experimental values of $\delta\Phi$ deviate from those predicted by Eq. 4. This discrepancy may be caused by the increase of electron-hole recombination in the superlattice layer at high P_B. When the heterojunction is irradiated with Light B, photo-excited electrons (holes) are driven towards the QW (GaAs buffer) by the built-in electric field (Fig. 3(b)). As P_B increases, the accumulation of holes in the GaAs buffer becomes more pronounced. The charge of accumulated holes weakens the built-in electric field. As a result, the recombination rate of holes increases before reaching the GaAs buffer, where Eq. 3 is no longer valid. This issue is important for improving the device performance and is left for future work.

3.3 Reliability of extracted Schottky barrier height

Before presenting the concluding remarks, we discuss the reliability of the extracted effective Schottky barrier height Φ and its reduction $\delta\Phi$ ($\equiv \Phi_0 - \Phi$). The absorbivity of aluminum has been reported to be around 8% for incident light with the wavelength range of 940 – 1064 nm.[26,27] Based on the Fresnel formula, the reflectance of a 100-nm-thick aluminum film is estimated to be around 94%. However, the actual optical absorptance is strongly affected by several factors, including the presence of an oxide layer, surface roughness, and contaminants,[28] making precise estimation difficult. Furthermore, in our experimental setup, Light A illuminates the entire heterojunction structure, including both the Schottky gate and ungated regions. Due to the high optical transparency of GaAs and AlGaAs crystals to Light A, a portion of the light incident on the ungated region may also reach the Schottky gate region by reflection at the back surface. This additional contribution further complicates the precise estimation of the optical absorptance A.

Rather than assuming the optical absorptance A a priori, we first estimated the effective Schottky barrier height Φ_0 (= 0.6 eV) under dark conditions based on the J_{SG}-V_G characteristics. We then compared Eq. (1) with the experimentally measured dependence of the photocurrent I_{SG} on the photon energy $h\nu_A$ in the absence of Light B (open circles in Fig. 8) to determine A. This analysis yielded $A \sim 0.042$ (4.2%), which was adopted in the previous section. However, in this procedure, imprecise evaluation of Φ_0 introduces errors in the extraction of A, potentially leading to considerable uncertainty in the determination of the Schottky barrier height Φ under illumination.

For intimate contacts with a clean interface, the Schottky barrier height Φ_0 between GaAs and Al has been reported to be 0.93±0.02 eV.[29] This value is frequently reduced due to interfacial contamination, the presence of an intermidiate insulating layer, or deep-level impurities. In studies of n-AlGaAs/GaAs field-effect transistors, Φ_0 is sometimes approximated as 0.7 eV.[30] Accordingly, we evaluate the optical absorptance A using Φ_0 = 0.7 eV instead of 0.6 eV, yielding $A \sim 0.061$ (6.1%). The Schottky photocurrent I_{SG} was then derived from Eq. (1), treating Φ as a fitting parameter following the approach in the previous section, with A set to ~ 0.061 instead of ~ 0.042 [Fig. 1(S) in Supplementary Data]. The dependence of I_{SG} on $h\nu_A$ remains well described by Eq. (1) even with $A \sim 0.061$, suggesting that the error in the value of Φ_0 has a minor effect on the overall agreement between Eq. (1) and the experimental data. The discrepancy observed in the previous section between the increasing and decreasing trends of I_{SG} with respect to $h\nu_A$ (P_B = 86 and 57 nW in Fig. 8) is slightly improved when the analysis is conducted using $A \sim 0.061$.

By contrast, the value of the Schottky barrier height Φ obtained through the fitting procedure is significantly affected by the estimation error of Φ_0 under dark conditions. We evaluated Φ under the assumption that Φ_0 is 0.5, 0.6, and 0.7 eV and found that the obtained Φ strongly depends on the assumed value of Φ_0 [Fig. 2(S) in Supplementary Data], implying that the extracted Φ values is not as reliable. This uncertainty can be effectively reduced by considering the Schottky barrier reduction $\delta\Phi$ ($\equiv \Phi_0 - \Phi$) [Fig. 3(S) in Supplementary Data], where the values of $\delta\Phi$ exhibit a dependence on P_B that is nearly independent of the assumed value of Φ_0. The result confirms that $\delta\Phi$ is a robust quantity, even when errors in Φ may be present.

4. Conclusions

The Schottky photocurrent I_{SG} in an n-AlGaAs/GaAs/AlGaAs double-heterojunction was studied for the irradiation of two light sources (Light A and B). Light A, which is a 940 nm, 975 nm, or 1064 nm laser, illuminates the entire Schottky gate region at an intensity of 60 μW/mm². Light B, a 670 nm laser, is used to locally illuminate the ungated region with a power P_B ranging from 0 to 2.9 μW. In the low P_B range (≤ 86 nA) and high P_B range (≥ 0.14 μW), I_{SG} exhibits an increase and decrease respectively with the increasing photon energy of Light A. By analyzing the experimental data using a hot carrier model, this behavior is well explained by the Schottky barrier lowering induced by Light B. As P_B increases, the reduction $\delta\Phi$ of the effective Schottky barrier height increases, where the maximum $\delta\Phi$ is about 0.5 – 0.6 eV.

References

1) R. Williams and R. H. Bube, J. Appl. Phys. **31**, 968 (1960).
2) W. G. Spitzer, C. R. Crowell, and M. M. Atalla, Phys. Rev. Lett. **8**, 57 (1962).
3) D. W. Peters, Proc. IEEE **55**, 204 (1967).
4) F. D. Shepherd, A. C. Yang, and R. W. Taylor, Proc. IEEE **58**, 1160 (1970).
5) E. Elabd, T. Villani, and W. Kosonocky, IEEE Electron Devices Lett., **3**, 89 (1982).
6) W. F. Kosonocky, F. W. Shallcross, T. S. Villani, and J. V. Groppe, IEEE Trans. Electron Devices, **32**, 1564 (1985).
7) J. M. Mooney, J. Appl. Phys. **65**, 2869 (1989).
8) B. Y. Tsaur, C. K. Chen, and J. P. Mattia, IEEE Trans. Electron Devices **11**, 162 (1990).
9) C. K. Chen, B. Nechay, and B. Y. Tsaur, IEEE Trans. Electron Devices **38**, 1094 (1991).
10) T. A. Yost, A. Madjar, and P. R. Herezfeld, IEEE Transactions on Microwave Theory and Techniques **49**, 1900 (2001).
11) M. Casalino, L. Sirleto, L. Moretti, and I. Rendina, Semicond. Sci. Technol. **23**, 075001 (2008).
12) M. Casalino, L. Sirleto, L. Moretti, M. Gioffrè, G. Coppola, and I. I. Rendina, Appl. Phys. lett. **92**, 251104 (2008).
13) S. Zhu, M. B. Yu, G. Q. Lo, and D. L. Kwong, Appl. Phys. Lett. **92**, 081103 (2008).
14) A. Akbari and P. Berini, Appl. Phys. Lett. **95**, 021104 (2009).
15) P. Berini, Adv. Opt. Photonics **1**, 484 (2009).
16) C. Scales, I. Breukelaar, and P. Berini, Opt. Lett. **35**, 529 (2010).
17) C. Scales and P. Berini, IEEE J. Quantum Electron. **46**, 633 (2010).
18) T. Kawazu, T. Noda, Y. Sakuma, and H. Sakaki, Appl. Phys. Lett., **106**, 022103, (2015).
19) T. Kawazu, T. Noda, and Y. Sakuma, Jpn. J. Appl. Phys. **56**, 04CG04, (2017).
20) T. Kawazu, T. Noda, and Y. Sakuma, Appl. Phys. Lett., **112**, 072101, (2018).
21) T. Kawazu, T. Noda, and Y. Sakuma, Jpn. J. Appl. Phys. **58**, SIIB05, (2019).
22) T. Kawazu, Jpn. J. Appl. Phys. **59**, 124003, (2020).
23) T. Kawazu, AIP Advances **14**, 125007, (2024).
24) E. Spenke, *Electronic Semiconductors* (McGraw-Hill, New York, 1958).
25) W. P. Dumke, Phys. Rev. **124**, 1813 (1961).
26) Bass M. Handbook of optics, Vol. 1, 2nd ed. (McGraw-Hill, New York, 1995).
27) L. Tunna, W. O'Neill, A. Khan, and C. Sutcliffe, Opt. Lasers Eng. 43, 937 (2005).
28) K. Howard, S. Lawson and Y. Zhou, Welding Journal 85 (5), 101 (2006).
29) S. M. Sze, *Physics of Semiconductor Devices* (Wiley, New York, 1981).
30) J. H. Davies, *The Physics of Low-dimensional Semiconductors* (Cambridge University Press, Cambridge, 1998)

Figure Captions

Fig. 1. Schematic drawing of sample cross-sectional view.

Fig. 2. Schematic drawings of the cross-section view (a) and the band diagram of n-AlGaAs/GaAs/AlGaAs double-heterojunction (b) when Light A is irradiated.

Fig. 3. Schematic drawings of the cross-section view (a) and the band diagram of n-AlGaAs/GaAs/AlGaAs double-heterojunction (b) when Light B is irradiated.

Fig. 4. Schematic drawing of Hall bar structure.

Fig. 5. Photocurrent I_{SG} for on/off action of Light A and B.

Fig. 6. Photocurrent I_{SG} for on/off action of Light A and B.

Fig. 7. Photocurrent I_{SG} for on/off action of Light A and B.

Fig. 8. Photocurrent I_{SG} as a function of photon energy $h\nu_A$ of Light A.

Fig. 9. Effective Schottky barrier height as a function of power P_B of Light B.

Fig. 10. Schottky barrier reduction $\delta\Phi$ as a function of power P_B of Light B.

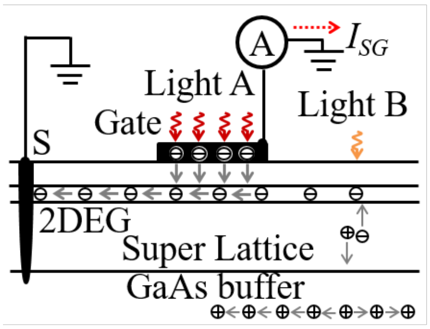

Fig.1.

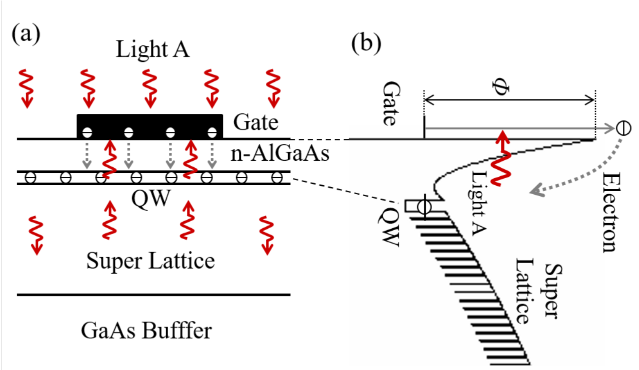
(a)
Light A
Gate
n-AlGaAs
QW
Super Lattice
GaAs Bufffer
(b)
Gate
Φ
Electron
Light A
QW
Super Lattice

Fig.2.

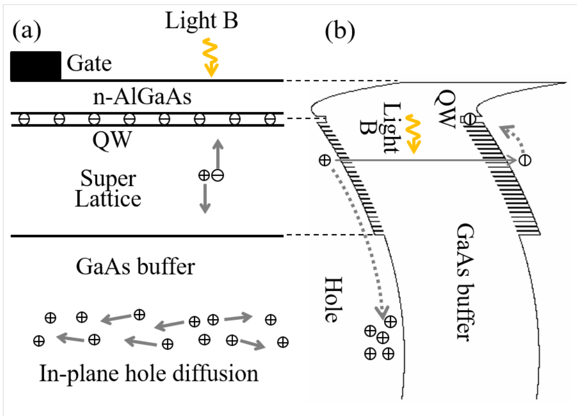
(a)
Light B
Gate
n-AlGaAs
QW
Super Lattice
GaAs buffer
In-plane hole diffusion
(b)
QW
Light B
Hole
GaAs buffer

Fig.3.

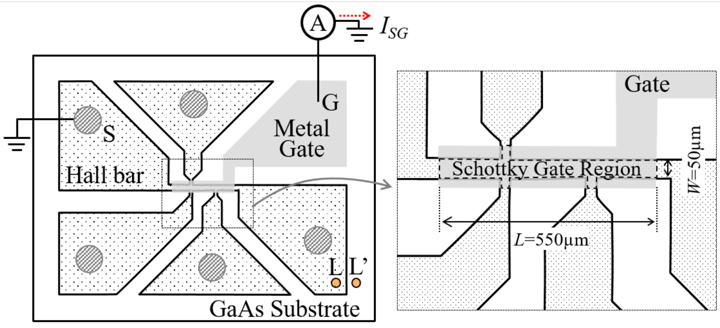

A
I_{SG}
G
S
Metal
Gate
Hall bar
L
L'
GaAs Substrate
Gate
Schottky Gate Region
W=50μm
L=550μm

Fig.4.

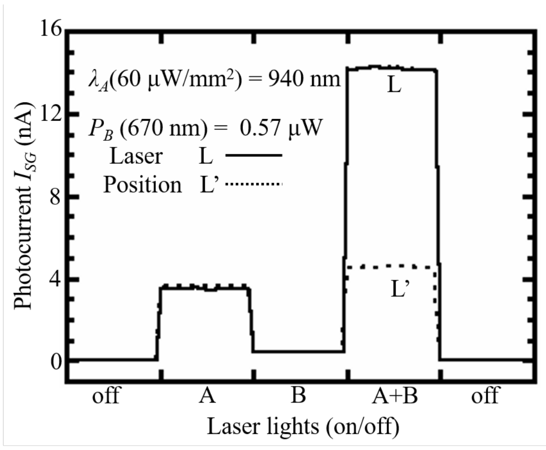

16
12
8
4
0
Photocurrent I_{SG} (nA)
λ_A(60 μW/mm^2) = 940 nm
P_B (670 nm) = 0.57 μW
Laser L
Position L'
L
L'
off
A
B
A+B
off
Laser lights (on/off)

Fig.5.

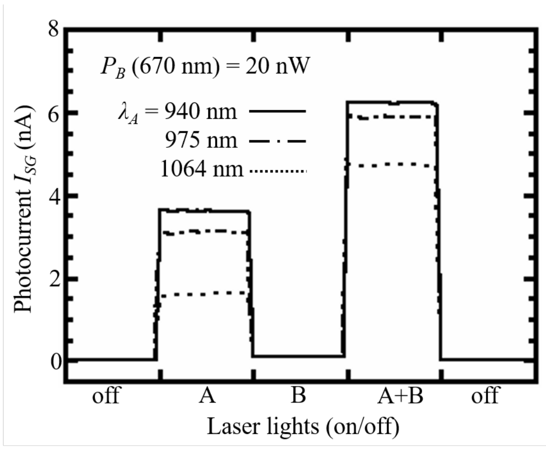

P_B (670 nm) = 20 nW
λ_A = 940 nm
975 nm
1064 nm
Photocurrent I_{SG} (nA)
0
2
4
6
8
off
A
B
A+B
off
Laser lights (on/off)

Fig.6.

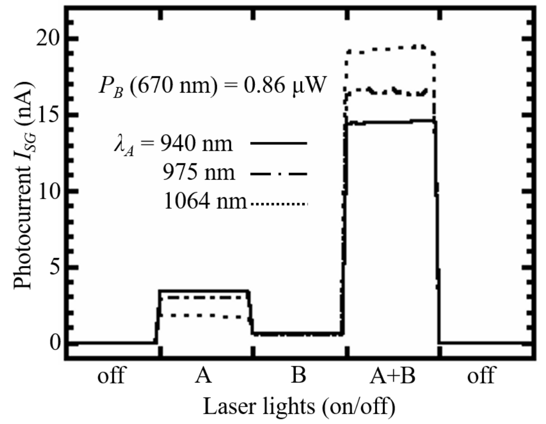

P_B (670 nm) = 0.86 µW
λ_A = 940 nm
975 nm
1064 nm
Photocurrent I_{SG} (nA)
20
15
10
5
0
off
A
B
A+B
off
Laser lights (on/off)

Fig.7.

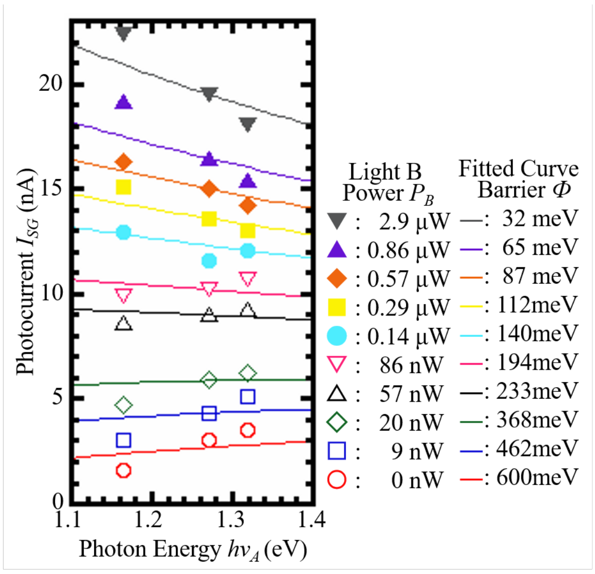

20
15
10
5
0
1.1
1.2
1.3
1.4
Photocurrent I_{SG} (nA)
Photon Energy $h\nu_A$ (eV)
Light B Power P_B
Fitted Curve Barrier Φ
: 2.9 μW —: 32 meV
: 0.86 μW —: 65 meV
: 0.57 μW —: 87 meV
: 0.29 μW —: 112meV
: 0.14 μW —: 140meV
: 86 nW —: 194meV
: 57 nW —: 233meV
: 20 nW —: 368meV
: 9 nW —: 462meV
: 0 nW —: 600meV

Fig.8.

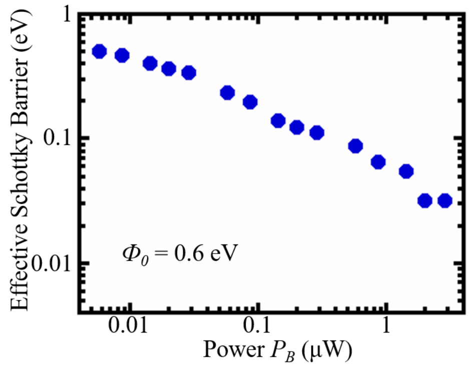
Effective Schottky Barrier (eV)
1
0.1
0.01
Φ_0 = 0.6 eV
0.01
0.1
1
Power P_B (μW)

Fig.9.

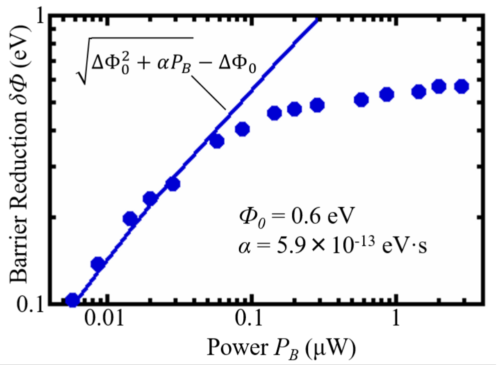
1
0.1
0.01
0.1
1
Barrier Reduction δΦ (eV)
Power P_B (μW)
$\sqrt{\Delta\Phi_0^2 + \alpha P_B} - \Delta\Phi_0$
Φ_0 = 0.6 eV
α = 5.9 × 10^-13 eV·s

Fig.10.